Ionization Energies and Dyson Orbitals of Thymine and Other Methylated Uracils†

O. Dolgounitcheva, V. G. Zakrzewski, and J. V. Ortiz*

Department of Chemistry, Kansas State University Manhatttan, Kansas 66506-3701

Received: January 11, 2002; In Final Form: April 1, 2002

Electron propagator methods are applied to the calculation of photoelectron spectra of thymine and other C- and N-methylated uracils. The Partial Third-Order electron propagator method is used. Excellent agreement with existing experimental spectra is achieved. Relationships between reductions in ionization energies and antibonding contributions from methyl groups in corresponding Dyson orbitals are discussed.

Introduction

Photoionization is the initial event in a variety of complex processes that lead to radiation damage of genetic material.[1,2] Methylation of nucleotides is considered to contribute to mutagenesis and carcinogenesis.[3−5] The presence of an electrophilic group, such as methyl, changes electron-donating properties of nucleobases. Photoelectron spectroscopy is among the most incisive probes of changes in electronic structure that accompany methylation of nucleobases.

Photoelectron spectra (PES) of gas-phase, nucleic-acid bases have been available for at least 25 years.[6−15] Assignments of the earlier spectra were done with the help of semiempirical methods, whereas in later works, ab initio calculations in rather small basis sets were employed. The role of configuration interaction in determining the order of the final states was considered in calculations employing Gaussian lobe basis sets.[16] Recently, the first vertical and adiabatic ionization energies (IEs) of the major forms of the four DNA bases were calculated with the B3LYP density functional model and the 6-31G* basis set as the energy differences between the ground and lowest ionized states.[17] Calculated IEs were systematically lower than the cited experimental data by 0.20−0.34 eV. A semiempirical AM1 variant of the Outer Valence Green Function was employed to obtain the first IE values of a number of isomers of DNA bases.[18] ΔSCF AM1 values were published in the same work.

Results of ab initio electron propagator calculations in the Partial Third Order (P3) approximation[19] with the 6-311G** basis[20] were recently published for uracil,[21] adenine,[21] guanine,[22] and 9-methylguanine.[23] Excellent agreement with existing experimental PES was achieved.

Of all the nucleic acid bases, only uracil and thymine do not have tautomers that are close in energy to the major forms occurring in nucleotides.[24] Thus, PES obtained for methylated uracil and thymine will not be obscured by the presence of tautomers. He(I) PES of thymine have been published in several papers.[7−12] Only one work contained spectra of other methylated uracils, ref 9.

Here, we present the results of ab initio, electron propagator calculations on the vertical IEs of thymine and other methyl uracils.

Methods

The P3 electron propagator approximation[19] has been reviewed recently.[23,25] This method has been successfully applied to many organic molecules[21,22,26] and has proved itself to be a reliable and inexpensive tool for assignment and interpretation of PES. For vertical IEs below 20 eV of closed-shell molecules, its average error is approximately 0.2 eV.[19, 26] This method has been incorporated into the Gaussian-98 suite of programs.[27]

In electron propagator calculations,[28,29] a pseudoeigenvalue problem is solved where

$$[\hat{F} + \hat{\Sigma}(E)]\psi^{\mathrm{Dyson}} = \epsilon\psi^{\mathrm{Dyson}}$$

The generalized Fock operator, $\hat{F}$, is supplemented by the energy-dependent, nonlocal, self-energy operator, $\hat{\Sigma}(E)$, which describes relaxation and correlation effects. To every IE, ϵ, there corresponds a Dyson orbital defined by

$$\psi^{\mathrm{Dyson}}(x_1) = \int \Psi_{\mathrm{neutral}}(x_1, x_2, x_3, ..., x_N)\Psi^*_{\mathrm{cation}} (x_2, x_3, x_4, ..., x_N)dx_2dx_3dx_4...dx_N$$

where the product between the N-electron, neutral wave function and the complex conjugate of the (N-1)-electron, cationic wave function is integrated over all electronic coordinates except x_1. In the P3 approximation to $\hat{\Sigma}(E)$ employed here, each Dyson orbital is proportional to a canonical, Hartree−Fock orbital, for nondiagonal couplings between the latter orbitals are neglected. The square of this proportionality factor is known as the pole strength. In the present calculations, all pole strengths are between 0.87 and unity. (The latter limit pertains to the case where correlation and relaxation corrections to Koopmans's theorem results vanish.) Such values validate the use of perturbative methods such as P3.

Molecular geometries were optimized with MBPT(2) total energies[30] and the 6-311G** basis. The same basis was used in electron propagator calculations at the optimized geometries.

All calculations in this work were performed with GAUSSIAN-98.[27] Molecular diagrams and orbital plots were graphed by MOLDEN.[31]

Results and Discussion

Structures. All possible rotational conformers were considered. Figure 1 contains the atomic numbering scheme. All

† Part of the special issue "Donald Setser Festschrift".

* To whom correspondence should be addressed. E-mail: ortiz@ksu.edu.

10.1021/jp020080o CCC: $22.00
Published on Web 05/09/2002

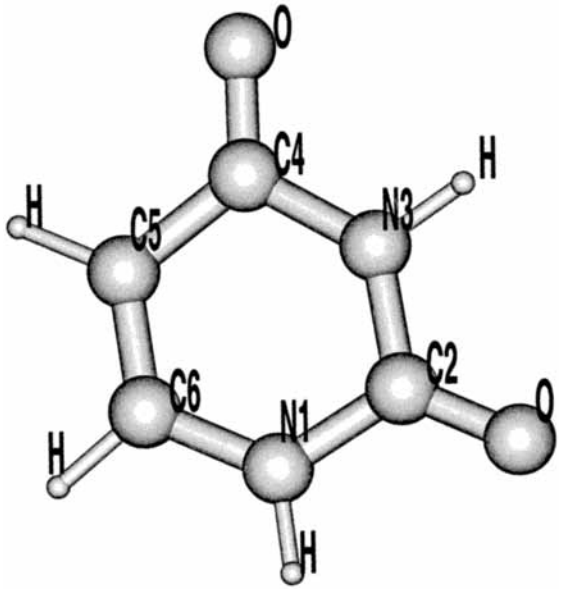

Figure 1. Atomic numbering scheme for uracil and methyl uracils.

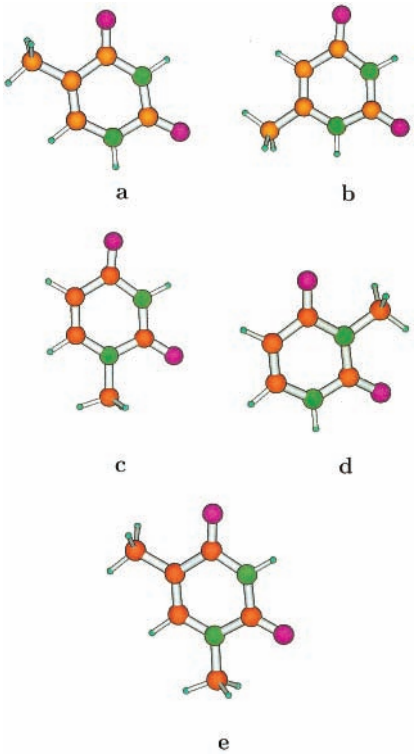

Figure 2. Molecular diagrams of methyl uracils: (a) Thymine, (b) 6-methyluracil, (c) N_1-methyluracil, (d) N_3-methyluracil, and (e) N_1-methylthymine (N_1, C_5-dimethyluracil).

minimum structures exhibit Cs symmetry. Optimized structures are presented in Figure 2. Bond lengths and angles are given in Tables 1 and 2.

The following notation is used henceforth. In the cis conformation of thymine (Figure 2a), one of methyl hydrogens lies in the ring plane and is in a cis position toward C_6, whereas the trans conformation corresponds to the opposite orientation of the same methyl hydrogen. For C_6-methyl uracil, a cis conformation is assigned to the structure with an in-plane H atom directed toward N_1. A trans conformation (Figure 2b) corresponds to the opposite orientation of the methyl group. N_1-methyl uracil displayed two possible conformations: cis corresponds to an in-plane H atom oriented toward C_6 (Figure 2c) and trans is the opposite case. For N_3-methyl uracil, cis designates a conformer with the in-plane methyl hydrogen oriented toward C_2 (Figure 2d) and trans corresponds to the opposite orientation. Four possible orientations of methyl groups were considered in N_1,C_5-dimethyl uracil. In each case, a cis orientation corresponds to either in-plane methyl hydrogen directed toward C_6. The trans-cis notation designates the N_1-methyl group in a trans orientation and C_5-methyl in a cis orientation. Figure 2e displays the cis−cis structure.

Total energies of all minima (min) and transition states (TS) are presented in Tables 3 and 4. Note that N_3-methyl uracil has two minima. For N_1,C_5-dimethyl uracil, the cis−cis and trans−cis minima have nearly identical energies.

TABLE 1: Optimized Bond Lengths in Methyl Uracils, Å

	thym	*trans*-C6	*cis*-N1	*cis*-N3	*cis- cis*-N1,C5
N_1C_2	1.387	1.391	1.394	1.391	1.390
C_2N_3	1.388	1.384	1.384	1.392	1.386
N_3C_4	1.404	1.408	1.408	1.414	1.402
C_4C_5	1.466	1.459	1.457	1.458	1.462
C_5C_6	1.355	1.356	1.355	1.351	1.358
N_1C_6	1.379	1.381	1.374	1.372	1.378
C_2O	1.214	1.214	1.217	1.217	1.218
C_4O	1.220	1.218	1.218	1.221	1.221
N_1C_{Me}			1.459		1.460
N_3C_{Me}				1.463	
C_5C_{Me}	1.499				1.499
C_6C_{Me}		1.499			
N_3H	1.013	1.013	1.013		1.013
N_1H	1.009	1.010		1.009	
C_5H		1.082	1.081	1.081	
C_6H	1.086		1.085	1.085	1.086
$C_{Me}H_a$[a]	1.093	1.090	1.090	1.087	1.090
$C_{Me}H_b$[a]	1.094	1.095	1.092	1.091	1.092
$C_{Me}H_{a1}$[b]					1.093
$C_{Me}H_{b1}$[b]					1.094

[a] H_a is an in-plane methyl group hydrogen, H_b is an out-of-plane methyl group hydrogen. [b] Pertains to the C5-methyl group in N1,C5-dimethyl uracil.

TABLE 2: Optimized Bond Angles in Methyl Uracils, deg

	thym	*trans*-C_6	*cis*-N_1	*cis*-N_3	*cis- cis*-N_1,C_5
$\angle N_1C_2N_3$	112.2	112.5	113.6	113.5	113.4
$\angle C_2N_3C_4$	128.8	128.5	129.1	126.3	128.9
$\angle N_3C_4C_5$	114.1	113.2	112.4	114.8	113.5
$\angle C_4C_5C_6$	118.4	120.9	120.0	119.9	118.5
$\angle C_5C_6N_1$	122.5	120.1	123.1	121.0	123.7
$\angle C_6N_1C_2$	124.1	124.8	121.7	124.5	122.0
$\angle N_1C_2O$	123.6	123.1	122.4	121.7	122.8
$\angle N_3C_4O$	121.0	120.7	120.9	120.0	121.1
$\angle C_2N_1C_{Me}$			116.2		116.2
$\angle C_2N_3C_{Me}$				117.8	
$\angle C_6C_5C_{Me}$	123.9				123.6
$\angle C_5C_6C_{Me}$		124.4			
$\angle C_2N_1H$	115.0	114.6		114.4	
$\angle C_2N_3H$	115.2	115.2	114.8		115.0
$\angle C_6C_5H$		121.2	121.3	122.0	
$\angle C_5C_6H$	122.2		121.9	123.2	121.4
$\angle N_1C_{Me}H_a$[a]			108.3		108.3
$\angle N_1C_{Me}H_b$[a]			110.2		110.2
$\angle N_3C_{Me}H_a$				107.8	
$\angle N_3C_{Me}H_b$[a]				109.5	
$\angle C_5C_{Me}H_a$	111.0				111.0
$\angle C_5C_{Me}H_b$	110.4				110.4
$\angle C_6C_{Me}H_a$		110.4			
$\angle C_6C_{Me}H_b$		110.4			

[a] H_a is an in-plane methyl group hydrogen, H_b is an out-of-plane methyl group hydrogen.

Ionization Energies

The following notations were used for combinations of oxygen, lone-pair contributions: subscript "-" designates an out-

TABLE 3: Methyl Uracil Total Energies +453. a.u.

N_1-cis	N_1- trans	N_3-cis	N_3-trans	C_5-cis	C_5-trans	C_6-cis	C_6- trans
−0.02057	−0.02006	−0.02097	−0.02094	−0.03309	−0.03081	−0.03255	−0.03509
min	TS	min	min	min	TS	TS	min

TABLE 4: N_1,C_5-dimethyl Uracil Total Energies +492. a.u.

cis−cis	cis−trans	trans−cis	trans−trans
−0.22266	−0.22044	−0.22231	−0.22009
min	TS	min	TS

TABLE 5: Uracil and Methyl Uracil Ionization Energies, EV

molecule	orbital	P3		PES[9]
Uracil	π_1	9.54		9.5
	σO_-	10.15		10.1
	π_2	10.52		10.6
	σO_+	11.12		11.2
	π_3	12.91		12.63
Thymine		cis	trans	
	π_1	9.14	9.11	∼9.1
	σO_-	9.95	10.09	∼10
	π_2	10.43	10.42	10.40
	σO_+	10.99	10.99	∼10.8−11.0
	π_3	12.52	12.52	12.30
C_6-methyl		cis	trans	
Uracil	π_1	9.19	9.27	∼9.3
	σO_-	9.92	9.95	∼9.7−10.2
	π_2	10.34	10.36	∼10.4
	σO_+	10.97	10.98	∼10.8−11.1
	π_3	12.36	12.32	12.13
N_1-methyl		cis	trans	
Uracil	π_1	9.14	9.18	∼9.20
	σO_-	10.00	10.01	∼9.9−10.05
	π_2	10.37	10.38	∼10.4
	σO_+	10.96	10.97	∼10.8−11.0
	π_3	12.38	12.32	∼12.10
N_3-methyl		cis	trans	
Uracil	π_1	9.37	9.37	∼9.2−9.5
	σO_-	9.96	9.97	∼10
	π_2	9.94	9.94	∼10
	σO_+	10.90	10.90	∼10.8−11
	π_3	12.47	12.45	12.27

TABLE 6: N_1,C_5-dimethyluracil Ionization Energies, eV

orbital type	cis−cis P3	cis−trans P3	trans−cis P3	trans−trans P3	PES9
π_1	8.78	8.76	8.76	8.80	∼8.8
σO	9.95	9.94	9.95	9.96	∼9.8−10.0[a]
π_2	10.28	10.27	10.27	10.28	∼10.3
σO	10.83	10.83	10.83	10.84	∼10.6−10.8[b]
π_3	12.04	12.03	12.03	11.95	11.72[c]

[a] A wide plateau with a peak at 10.0 eV. [b] A peak at ∼10.6 eV followed by a plateau to 10.8 eV. [c] No picture for this ionization in ref 9.

of-phase combination, whereas "+" is used for an in-phase combination.

IEs of all four methyl-substituted uracils are compiled in Table 5 together with those of uracil. IEs of N_1,C_5-dimethyl uracil are presented in Table 6. Figures 3−8 present ±0.05 contours of the Dyson orbitals. Relaxation and correlation corrections to the results of Koopmans's theorem are approximately 2 eV for the oxygen, lone-pair hole states, but are considerably smaller for the π final states. The order of final states predicted by canonical, Hartree−Fock orbital energies is π_1, π_2, n_1, n_2, and π_3 for all molecules. This sequence differs from the P3 predictions for all molecules except 3-methyl uracil.

Uracil. P3 IEs and Dyson orbitals (DOs) are reviewed here for the sake of comparison to other molecules. (An extensive discussion of the IEs of uracil can be found in ref 21.) The following IEs were predicted for uracil: 9.54, 10.15, 10.52, 11.12 and 12.91 eV. The first four values are in excellent agreement with available experimental data (see Table 5). The fifth IE, which pertains to a π_3 DO, is somewhat higher than the experimental value, however. This larger discrepancy is likely to be due to complex correlation effects that the P3 approximation does not describe well. (Extensive configuration mixing for this state was found in the Gaussian lobe calculations of ref 16 as well.) Similar trends have been observed previously in refs 26, parts d, g, j, and k. DO diagrams for uracil are presented in Figure 3. π_1 and π_2 DOs qualitatively confirm simple depictions of atomic orbital contributions to MOs in ref 9 that were based on semiempirical, CNDO calculations. The π_1 density is fairly delocalized over most heavy atoms with the largest contributions from a C_5C_6 bonding lobe and an N_1 atomic orbital with the opposite phase. In addition, there are two π lobes localized on both oxygens. The DO of the n_1 level, although dominated by oxygen contributions, is widely delocalized into the ring. Three lobes with alternating phases on the oxygens and N_3 obtain in the π_2 DO. Oxygen contributions predominate in the n_2, σO_+ orbital, but with the opposite phase relationship between the oxygen-centered lobes. For the π_3 DO, two, three-center π lobes have opposite phases. One of these lobes is delocalized over the $N_1C_6C_5$ fragment, whereas the other settles on the OCC_2N_3 region. C_4 participation is not important. The following order of P3 energies was obtained: π_1, n_1, π_2, n_2, and π_3.

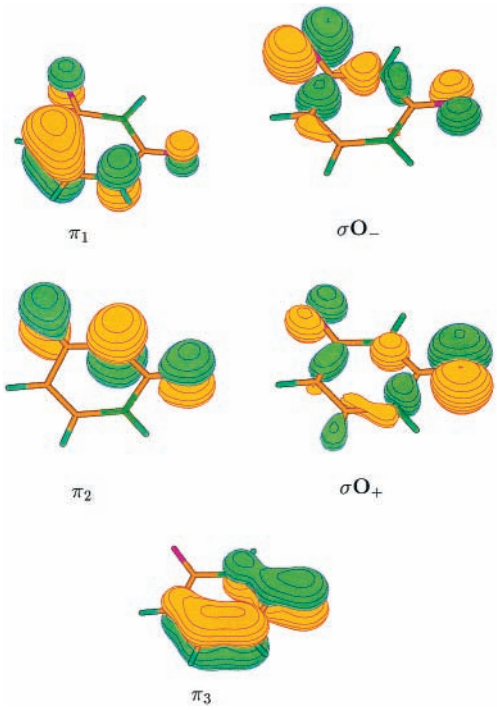

Figure 3. Uracil Dyson Orbitals.

C-methylated Uracils: Thymine and C_6-methyl Uracil. Only the cis conformer of thymine is a rotational minimum. Because the rotational barrier is only 1.43 kcal/mol, methyl group rotation is almost free. IEs of two rotamers of thymine are almost identical with the exception of the ionization from the σO_- orbital, for which a difference of 0.14 eV obtains. For the first four ionizations, very good correspondence with

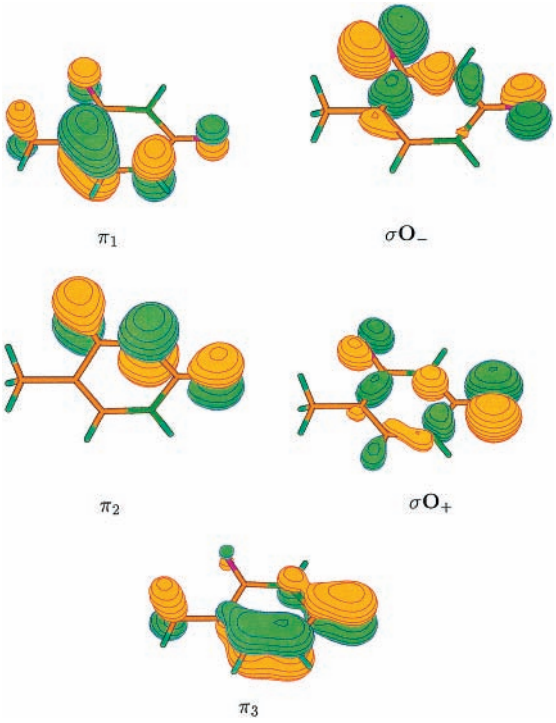

Figure 4. Thymine Dyson Orbitals.

experiment is achieved. The position of the fifth, π_3 band is predicted at higher energy than observed; larger discrepancies between theory and experiment are typical for higher, π-hole IEs.[21,22] The trends observed for experimental ionization energy shifts[8,9,11] are well reproduced in our P3 calculations. Maximum shifts of 0.4 eV were obtained for ionizations from π_1 and π_3 levels. The IE of a π_2 level changes only slightly, by 0.1 eV (0.2 eV in ref 9), while the IEs of two σ levels are affected by 0.06−0.20 eV. A comparison of the corresponding DO diagrams of uracil and thymine gives an explanation for this phenomenon (see Figure 4). All thymine DOs qualitatively resemble their uracil counterparts. The only two DOs with appreciable contribution from a methyl group are π_1 and π_3. In both cases, a pseudo-π lobe of CH_3 is in antibonding conjugation with the nearest C−C π binding lobe. No such interaction takes place for the σO or π_2 DOs.

A trans conformation of C_6-methyl uracil is a minimum and the rotational barrier in this system is assessed as 1.49 kcal/mol. P3 IEs for this conformation are in excellent agreement with experimental PES of ref 9. The first IE is only ∼0.2−0.3 eV lower than in the case of uracil and the DO for this level shows no participation from the methyl group (see Figure 5). The shift with respect to uracil for the next, σO_- level is essentially the same as for thymine and the respective DO does not show any changes. The same is true for the next two ionizations. For the π_3 case, however, the shift is much stronger than in thymine: 0.59 eV (P3) or 0.5 eV (PES). The corresponding DO has a marked antibonding relationship between the pseudo-π contribution of CH_3 and the $C_5C_6N_1$ lobe.

N-methylated Uracils: N_1- and N_3-methyl Uracils. A cis conformation of N_1-methyl uracil corresponds to a rotational minimum. The barrier to methyl group rotation is very low. P3 ionization energies of the *cis* and *trans* forms (a barrier top) are almost identical (see Table 5). In the experimental spectrum of N_1-methyl uracil, two IE values pertaining to π levels are significantly shifted to lower energy. Of these, the π_3 level is most significantly destabilized as the IE declines by ∼0.5 eV compared to uracil. The π_2 and both σ levels are shifted

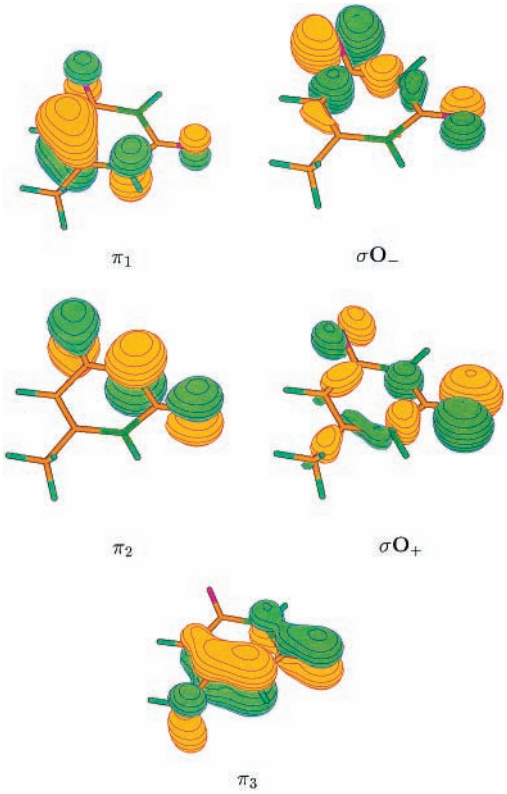

Figure 5. C_6-methyl Uracil Dyson Orbitals.

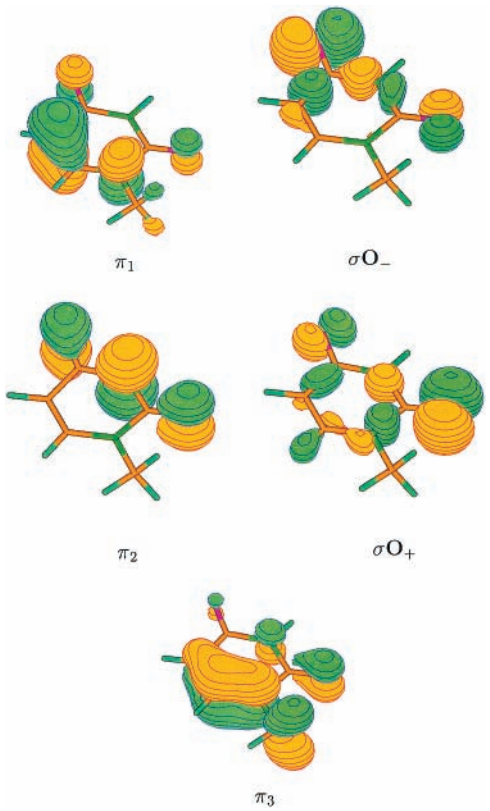

Figure 6. N_1-methyl Uracil Dyson Orbitals.

approximately to the same extent as the respective levels in thymine (that is, by no more than 0.2 eV). Once again, P3 results are in excellent agreement with the experimental peaks. σO_-, π_2 and σO_+ DOs are essentially the same as in uracil (Figure 6). In the π_1 DO, delocalization into the pseudo π lobes of CH_3 is somewhat less pronounced than in thymine. The π_3 DO is

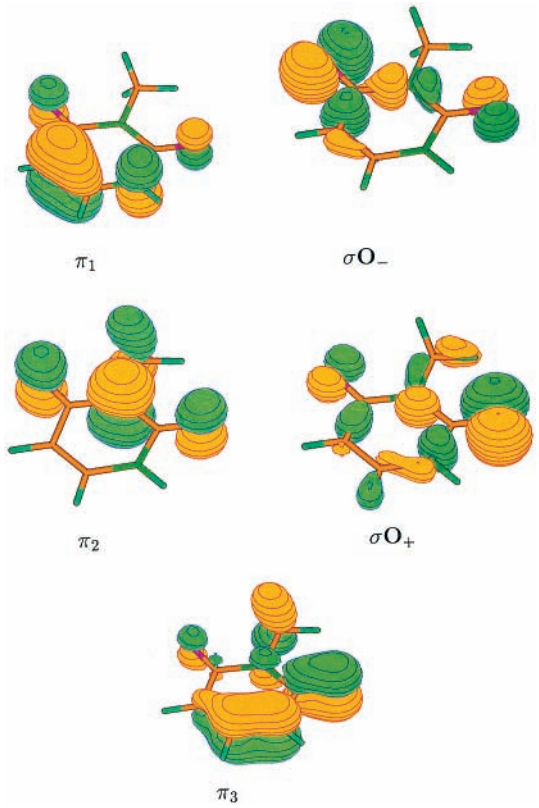

Figure 7. N_3-methyl Uracil Dyson Orbitals.

very strongly destabilized by antibonding, π conjugation between CH_3 and the nearest, three-center $C_5C_6N_1$ fragment. Additional destabilization might be caused by reduced bonding interaction in the N_3C_2O lobe (see Figures 3 and 6).

The PES of N_3-methyl uracil (see ref 9) is significantly different from the spectra of all the other methylated uracils. The first experimental band is flat and very wide covering the range of ~9.2−9.5 eV with no clear maximum. The next band covers ~9.5−10.2 eV and was assigned to two overlapping features, a peak at ~10.0 eV caused by electron removal from a π_2 level, and a smooth shoulder to the left of it which was assigned to ionization from a σO level. The following peak of low intensity at ~10.8 eV was assigned to ionization from another lone-pair level. The last IE under consideration was set at 12.27 eV and assigned to a π_3 level.

Two rotational minima were obtained in MBPT(2) optimizations of N_3-methyl uracil and their total energies differed only by 0.02 kcal/mol. The IEs are nearly identical (see Table 4). The first P3 IE value is 9.37 eV, which fits very well into the observed band. The π_1 amplitudes are almost exactly the same as in uracil (compare Figure 3 and Figure 7). There is no pseudo-π contribution from the methyl group and as a result, this π_1 level suffers the least destabilization by methylation of any molecule here. 9.96 eV is predicted as the IE from the σO_- level. This value is well within the second band of ref 9. As in all previous cases, the methyl group does not contribute to the DO and the resulting shift is small. In contrast to other methyl uracils, the π_2 level is shifted by ~0.6 eV with respect to uracil. P3 values are in excellent agreement with the experimental peak position. A large, pseudo-π methyl group contribution provides antibonding conjugation in the π_2 DO (Figure 7). The next IE is predicted at 10.90 eV. Once again, this value is in very good agreement with the experimental band position. The corresponding DO exhibits only small input from the methyl group, with one lobe in a bonding pattern with an oxygen lone-pair function and another lobe in an antibonding interaction with the other oxygen lone-pair pattern. The last P3 IE of 12.47 eV is a little higher than the experimental one, but the shift with respect to uracil is reproduced well. As was the case in N_1-methyl uracil, an appreciable contribution from a methyl group in an antibonding mode is observed in the corresponding π_3 DO (Figure 7). The bonding character of the N_3-C_2-O lobe is diminished as well.

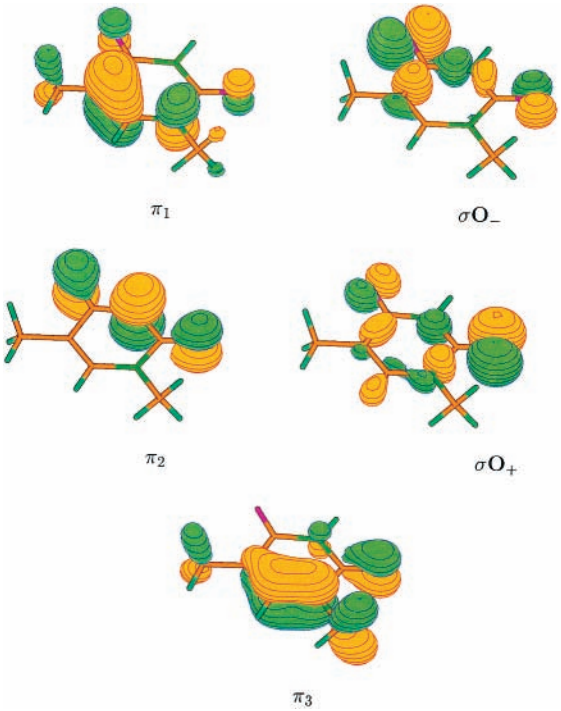

Figure 8. N_1-methyl Thymine Dyson Orbitals.

N_1-methylthymine (N_1,C_5-dimethyl Uracil). Four stationary points were obtained in optimizations of N_1,C_5-dimethyl uracil. Of these, the cis−cis and trans−cis conformations proved to be minima. The largest rotational barrier is estimated as 1.39 kcal/mol. P3 IEs do not change much due to rotation. The experimental PES of this dimethyl derivative of uracil consists of two distinctive areas: a wide, separately standing band with a diffuse maximum at ~8.8 eV and a very complicated energy region which results from a superposition of several bands. P3 results are in excellent agreement with experimental data for the first four ionizations. The fifth IE is about 0.3 eV higher than the IE reported in ref 9. The presence of two methyl groups leads to significant disturbances of π_1 and π_3 levels. Both methyl groups contribute to antibonding, pseudo-π conjugation in π_1, although N_1-methyl participation is less pronounced. No such interaction takes place for π_2 or either of the *n* levels and the corresponding shifts with respect to uracil are smaller. The strongest shift is observed for the π_3 level (0.87 eV with P3 versus 0.91 eV, experimental). The corresponding DO diagram (Figure 8) shows large antibonding contributions from both methyl groups and severely reduced bonding between C_2O and N_3.

Conclusions

Agreement between P3 electron propagator predictions and ionization energies inferred from photoelectron spectra is excellent. Correlated calculations are needed to produce the correct order of the final states. Figure 9 summarizes the shifts in IEs. In each molecule, the order of final states is π_1, σO_-, π_2, σO_+, and π_3. Where the amplitudes of the π_1 DO are most

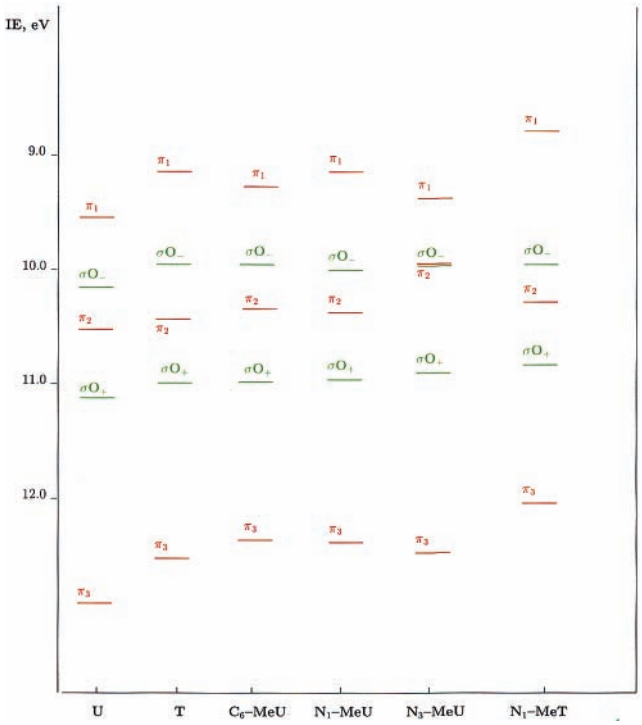

Figure 9. Summary of Ionization Energies

pronounced, the corresponding methyl substitutions on uracil have their greatest effects on the IEs and the DOs. Each of the IE shifts pertaining to thymine and the N_1-methyl isomer is approximately half the shift for the dimethylated species. Antibonding relationships between methyl groups and ring-centered lobes produce the lowered IEs. Similar arguments hold for the shifts of the π_3 IEs. The only substitution which is properly deployed to affect the π_2 level in a similar manner takes place at the N_3 position. Therefore, IE shifts in the π_2 levels are relatively small, except for the N_3-methyl isomer. In the remaining σ levels, the shifts are relatively minor. The preceding relationships between IE shifts and antibonding contributions from methyl groups to Dyson orbitals are based on correlated, ab initio, electron propagator calculations.

Acknowledgment. This work was supported by the National Science Foundation under Grant Nos. CHE-9873897 and CHE-0135823.

References and Notes

(1) Becker, D.; Sevilla, M. D. In *Advances in Radiation Biology Vol. 17*; Lett, J. T., Adler, H., Eds.; Academic Press: New York, 1993; pp. 121−180.

(2) Steenken, S. *Chem. Rev.* **1989**, *89*, 503.

(3) Kim, N. S.; Zhu, Q.; LeBreton, P. R. *J. Am. Chem. Soc.* **1999**, *121*, 11 516, and references therein.

(4) Zhu, Q.; LeBreton, P. R. *J. Am. Chem. Soc.* **2000**, *122*, 12 824 and references therein.

(5) Kim, N. S.; LeBreton, P. R. *J. Am. Chem. Soc.* **1996**, *118*, 3694.

(6) Hush, N. S.; Cheung, A. S. *Chem. Phys. Lett.* **1975**, *34*, 11.

(7) Lauer, G.; Schäfer, W.; Schweig, A. *Tetrahedron Lett.* **1975**, 3939.

(8) Dougherty, D.; Wittel, K.; Meeks, J.; McGlynn, S. P. *J. Am. Chem. Soc.* **1976**, *98*, 3815.

(9) Padva, A.; O'Donnell, T. J.; LeBreton, P. R. *Chem. Phys. Lett.* **1976**, *41*, 278.

(10) Padva, A.; Peng, S.; Lin, J.; Shahbaz, M.; LeBreton, P. R. *Biopolymers* **1978**, *17*, 1523.

(11) Urano, S.; Yang, X.; LeBreton, P. R. *J. Mol. Struct.* **1989**, *214*, 315.

(12) Kubota, M.; Kobayashi, T. *J. Electron Spectrosc. Relat. Phenom.* **1996**, *82*, 61.

(13) (a) Peng, S.; Padva, A.; LeBreton, P. R. *Proc. Natl. Acad. Sci. U.S.A.* **1976**, *73*, 2966. (b) Lin, J.; Yu, C.; Peng, S.; Akiyama, I.; Li, K.; Lee, L. K.; LeBreton, P. R. *J. Am. Chem. Soc.* **1980**, *102*, 4627.

(14) (a) Dougherty, D.; McGlynn, S. P. *J. Chem. Phys.* **1977**, *67*, 1289. (b) Lin, J.; Yu, C.; Peng, S.; Akiyama, I.; Li, K.; Lee, L. K.; LeBreton, P. R. *J. Phys. Chem.* **1980**, *84*, 1006.

(15) (a) Yu, C.; Peng, S.; Akiyama, I.; Lin, J.; LeBreton, P. R. *J. Am. Chem. Soc.* **1978**, *100*, 2303. (b) Dougherty, D.; Younathan, E. S.; Voll, R.; Abdulnur, S.; McGlynn, S. P. *J. Electron Spectrosc. Relat. Phenom.* **1978**, *13*, 379.

(16) O'Donnell, T. J.; LeBreton, P. R.; Petke, J. D.; Shipman, L. L. *J. Phys. Chem.* **1980**, *84*, 1975.

(17) Hutter, M.; Clark, T. *J. Am. Chem. Soc.* **1996**, *118*, 7574.

(18) Leão, M. B. C.; Longo, R. L.; Pavão, A. C. *J. Mol. Struct.* **1999**, *490*, 145.

(19) Ortiz, J. V. *J. Chem. Phys.* **1996**, *104*, 7599.

(20) (a) Krishnan, R.; Binkley, J. S.; Seeger, R.; Pople, J. A. *J. Chem. Phys.* **1980**, *72*, 650. (b) Petersson, G. A.; Bennett, A.; Tensfeldt, T. G.; Al-Laham, M. A.; Shirley, W. A.; Mantzaris, J. *J. Chem. Phys.* **1988**, *89*, 2193. (c) Petersson, G. A.; Al-Laham, M. A. *J. Chem. Phys.* **1991**, *94*, 6081.

(21) Dolgounitcheva, O.; Zakrzewski, V. G.; Ortiz, J. V. *Int. J. Quantum Chem.* **2000**, *80*, 831.

(22) Dolgounitcheva, O.; Zakrzewski, V. G.; Ortiz, J. V. *J. Am. Chem. Soc.* **2000**, *122*, 12 304.

(23) Ferreira, A. M.; Seabra, G.; Dolgounitcheva, O.; Zakrzewski, V. G.; Ortiz, J. V. In. *Quantum-Mechanical Prediction of Thermochemical Data*; Cioslowski, J., Ed.; Kluwer: Dordrecht, 2001, p 131.

(24) Leszczynski, J. In. *The Encyclopedia of Computational Chemistry*; John Wiley and Sons: New York, 1998; Vol. 5, p 2951.

(25) Ortiz, J. V.; Zakrzewski, V. G.; Dolgounitcheva, O. In. *Conceptual Trends in Quantum Chemistry*; Kryachko, E. S., Ed.; Kluwer: Dordrecht, 1997; Vol. 3, p 465.

(26) (a) Ortiz, J. V. *J. Chem. Phys.* **1996**, *104*, 7599. (b) Ortiz, J. V.; Zakrzewski, V. G. *J. Chem. Phys.* **1996**, *105*, 2762. (c) Zakrzewski, V. G.; Ortiz, J. V. *J. Phys. Chem.* **1996**, *100*, 13 979. (d) Zakrzewski, V. G.; Dolgounitcheva, O.; Ortiz, J. V. *J. Chem. Phys.* **1996**, *105*, 8748. (e) Zakrzewski, V. G.; Ortiz, J. V. *J. Mol. Struct.* **1996**, *388*, 351. (f) Ortiz, J. V. *Int. J. Quantum Chem.* **1997**, *63*, 291. (g) Dolgounitcheva, O.; Zakrzewski, V. G.; Ortiz, J. V. *J. Phys. Chem. A* **1997**, *101*, 8554. (h) Zakrzewski, V. G.; Dolgounitcheva, O.; Ortiz, J. V. *J. Chem. Phys.* **1997**, *107*, 7906. (i) Zakrzewski, V. G.; Dolgounitcheva, O.; Ortiz, J. V.; Ratovski, G. V. *Int. J. Quantum Chem.* **1998**, *70*, 1037. (j) Zakrzewski, V. G.; Dolgounitcheva, O.; Ortiz, J. V. *Int. J. Quantum Chem.* **1999**, *75*, 607. (k) Dolgounitcheva, O.; Zakrzewski, V. G.; Ortiz, J. V. *J. Phys. Chem. A* **2000**, *104*, 10 032.

(27) Frisch, M. J.; Trucks, G. W.; Schlegel, H. B.; Scuseria, G. E.; Robb, M. A.; Cheeseman, J. R.; Zakrzewski, V. G.; Montgomery, J. A., Jr.; Stratmann, R. E.; Burant, J. C.; Dapprich, S.; Millam, J. M.; Daniels, A. D.; Kudin, K. N.; Strain, M. C.; Farkas, O.; Tomasi, J.; Barone, V.; Cossi, M.; Cammi, R.; Mennucci, B.; Pomelli, C.; Adamo, C.; Clifford, S.; Ochterski, J.; Peterson, G. A.; Ayala, P. Y.; Cui, Q.; Morokuma, K.; Malick, D. K.; Rabuck, A. D.; Raghavachari, K.; Foresman, J. B.; Cioslowski, J.; Ortiz, J. V.; Stefanov, B. B.; Liu, G.; Liashenko, A.; Piskorz, P.; Komaromi, I.; Gomperts, R.; Martin, R. L.; Fox, D. J.; Keith, T.; Al-Laham, M. A.; Peng, C. Y.; Nanayakkara, A.; Gonzalez, C.; Challacombe, M.; Gill, P. M. W.; Johnson, B.; Chen, W.; Wong, M. W.; Andres, J. L.; Head-Gordon, M.; Replogle, E. S.; Pople, J. A. *Gaussian 98*, Revision A7, Gaussian, Inc., Pittsburgh, PA, 1998.

(28) Ortiz, J. V. In *Computational Chemistry: Reviews of Current Trends, Vol. 2*; Leszczynski, J., Ed.; World Scientific: Singapore, 1977; p. 1.

(29) Ortiz, J. V. *Adv. Quantum Chem.* **1999**, *35*, 33 and references therein.

(30) Bartlett, R. J. *Annu. Rev. Phys. Chem.* **1981**, *32*, 359 and references therein.

(31) Schaftenaar, G. MOLDEN 3.4, CAOS/CAMM Center, The Netherlands, 1998.